

## Global Observables at RHIC

Peter A. Steinberg<sup>a</sup>

<sup>a</sup> Brookhaven National Laboratory  
Upton, NY 11973

The first three measurements from the RHIC program were results on global observables: charged particle multiplicity ( $N_{ch}$ ), transverse energy ( $E_T$ ) and elliptic flow ( $v_2$ ). They offer a look at the large-scale features of particle production in high-energy nuclear collisions, with particular insight into entropy production and collective behavior. Results from all of the RHIC experiments are discussed in light of data from lower energy nuclear collisions as well as from high-energy hadronic collisions to test our current understanding of the collision dynamics.

### 1. Introduction

It is hoped that Au+Au collisions at RHIC will form a large, collective state of thermally equilibrated matter. Such a state should be describable by simple quantities, such as energy density and pressure, which can be related to lattice or hydrodynamic calculations incorporating a nuclear equation of state. One means to study this is to measure global quantities that characterize the entire event. Looking along the beam axis, we can attempt to understand the energy density achieved in the collision by studying the multiplicity and  $E_T$  distributions ( $dN_{ch}/d\eta$ ,  $dE_T/d\eta$ ). These can also be compared with  $pp$ ,  $\bar{p}p$  and  $pA$  collisions at higher and lower energies to study their scaling with the number of participating nucleons as well as the number of binary collisions. Azimuthal distributions in slices of  $\eta$ , studied by means of their Fourier coefficients, can be compared with results from lower energy nuclear collisions, where a steady increase of  $v_2$  with energy has been observed. This indicates that the particle emission becomes increasingly ellipsoidal, suggesting increased transverse pressure. Taken together, these measurements offer the first look at collective particle production and dynamics at RHIC. It is an open question, however, whether features of the initial state can survive the hadronization process. We review the data discussed at Quark Matter 2001 [1] to test our understanding of how the dynamics of the early stages of RHIC collisions can be observed in the final state.

### 2. Centrality

To understand whether particle production in nuclear collisions is fundamentally different than in  $pp$  or  $pA$  collisions, it is important to understand the collision geometry. The impact parameter of the collision determines  $N_{part}$ , the number of nucleons that interact inelastically (i.e. participate), as well as  $N_{spec}$ , the number of spectator nucleons which

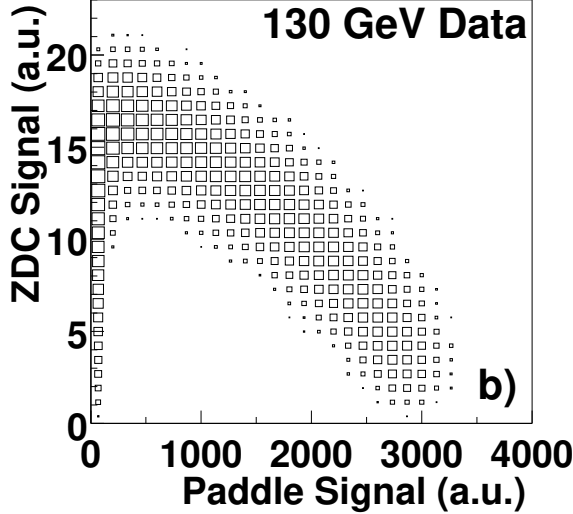


Figure 1. Correlation between the ZDC energy and multiplicity between  $3 < |\eta| < 4.5$  (from PHOBOS).

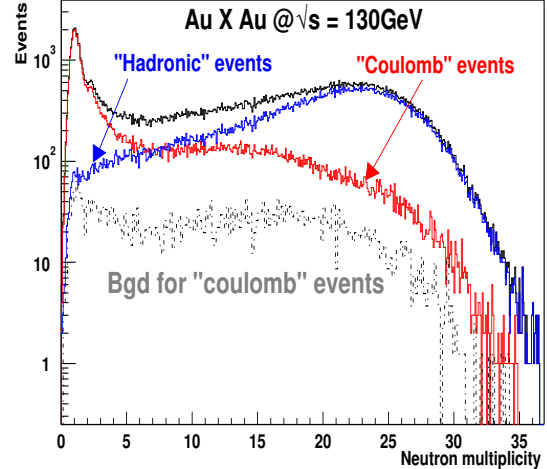


Figure 2. Spectrum of a single ZDC detector (from PHENIX).

do not interact and continue along the beam direction. To determine  $N_{part}$  in fixed target experiments, a zero-degree calorimeter (ZDC) is used to measure the forward energy and directly infer  $N_{part}$  by the relationship  $N_{part} + N_{spec} = 2A$ . At RHIC, each experiment is equipped with a pair of ZDCs[2] placed behind dipole magnets which sweep away charged particles and nuclear fragments, leaving primarily spectator neutrons. Figure 1 shows PHOBOS data on the relationship between charged particle production in  $3 < |\eta| < 4.5$  and the neutral energy measured by the RHIC ZDCs. This data suggests that above a certain  $N_{part}$ , the number of produced particles is in fact monotonically related to  $N_{part}$ .

Although one cannot directly measure the number of participants in a given collision, one can use this monotonic relationship of  $N_{part}$  with respect to  $N_{ch}$  or  $E_T$  to relate a fraction of the cross section to a range in  $N_{part}$ . This is done by means of the Glauber model of nuclear collisions [3,4], which allows the calculation of  $N_{part}$  as well as the number of binary collisions,  $N_{coll}$ , experienced by the colliding system as a function of the impact parameter.

Of course, any attempt to measure a fraction of the total inelastic cross section is necessarily limited by an experiment's understanding of its trigger efficiency, since the systematic error increases for more peripheral events. This is complicated by the fact that the ZDCs are sensitive to mutual Coulomb dissociation[5], as seen in Figure 2 from PHENIX. However, theoretical calculations are available and current comparisons of data and theory [5–7] are in good agreement.

Despite the difficulties in doing so, there are real benefits in estimating  $N_{part}$  and  $N_{coll}$ . Scaling  $pA$  and  $AA$  results by  $N_{part}$  allows the comparison of results to  $pp$  data. Also, experimentalists can correct for the effects of fluctuations due to physics effects or detector acceptance which bias the measurement of the actual nuclear geometry. This facilitates making reliable comparisons of the RHIC experiments to each other and to SPS and AGS

data.

### 3. Charged Particle Multiplicity

The multiplicity of charged particles produced in heavy ion collisions arises from a variety of physics processes. In addition to the expected soft processes seen at lower energies, hard processes, nuclear shadowing, and hadronic rescattering all play a role[9]. Each of these has an effect on the number of degrees of freedom available to the colliding system (i.e. the entropy). Although a value of  $N_{ch}$  in isolation does not provide insight into the relative contributions of the various processes, we can attempt to disentangle them by systematically varying the initial conditions of the collision and comparing the results to  $pp$  and  $pA$  data as well as theoretical models. For this, it is useful to study the charged particle multiplicity per participant pair,  $dN_{ch}/d\eta/\frac{1}{2}N_{part}$ .

Theoretical models of particle production in RHIC collisions broadly fall into two classes (see [8]). The first class is based on modifying the wounded nucleon model to include hard processes. In these, one assumes that hard and soft processes scale with binary collisions and wounded nucleons, respectively:  $dN_{ch}/d\eta = A \times N_{part} + B \times N_{coll}$ . Both HIJING [9,10] and the eikonal model proposed by Kharzeev and Nardi (KN) [4] follow this approach. However, while HIJING includes additional physics effects (jet quenching and nuclear shadowing) which lead to a linear rise in  $dN_{ch}/d\eta/\frac{1}{2}N_{part}$  vs.  $N_{part}$ , the KN calculation only uses as input the fraction of hard processes and the PHOBOS result. This leads to a dependence of  $dN_{ch}/d\eta$  similar to that measured by WA98[13] and WA97[14] which is well described by a simple power-law form,  $CN_{part}^\alpha$ .

The other class of calculations, based on parton saturation, predict a very different dependence on  $N_{part}$ . EKRT [15,8] found that a geometry-dependent saturation scale predicts a nearly-constant dependence of  $dN_{ch}/d\eta/\frac{1}{2}N_{part}$  as a function of  $N_{part}$ . Kharzeev and Nardi [4] also perform a calculation based on parton saturation, including the running of the strong coupling constant with saturation scale, that finds  $dN_{ch}/d\eta$  per participant to scale as  $\ln(Q_s^2/\Lambda^2)$ , where  $Q_s^2$  is the impact-parameter dependent saturation momentum scale. This result agrees well with their eikonal calculation, perhaps fortuitously.

Before comparing these predictions with experimental data, it is important to make sure that both theory and experiment are discussing the same quantity. To convert  $dN_{ch}/dy$  to  $dN_{ch}/d\eta$ , it is not correct simply to apply a global correction factor, e.g. 95%. Rather, one must apply the proper Jacobian,  $dy = \beta d\eta$ , to the  $dN_{ch}/dy$  distribution for each species of charged particle to transform it to  $dN_{ch}/d\eta$ . It is useful to expand this expression,

$$\frac{dN}{d\eta} = \frac{dN}{dy} \sqrt{1 - \left( \frac{m}{m_T \cosh y} \right)^2}, \quad (1)$$

where we see that the two distributions converge at large  $y$  and  $m_T$ . Thus,  $dN_{ch}/d\eta$  near mid-rapidity generally agrees with  $dN_{ch}/dy$  at fixed-target experiments at CERN, but significant deviations ( $\sim 15\%$ ) arise at collider experiments, even for lighter species like pions.

The first published results from RHIC were the measurement of  $dN_{ch}/d\eta|_{\eta=0}/\frac{1}{2}N_{part}$  as a function of energy [12], shown in Figure 3. This provided the first opportunity to compare extrapolations of  $pp$  and  $\bar{p}p$  collisions to  $AA$  collisions at the highest available

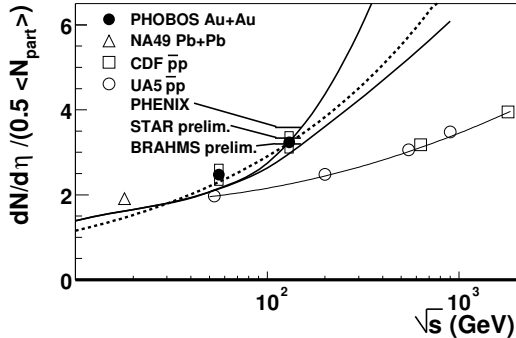


Figure 3. Energy dependence of  $dN_{ch}/d\eta|_{|\eta|<1/2 N_{part}}$  with results from all four RHIC experiments at  $\sqrt{s_{NN}} = 130$  GeV.

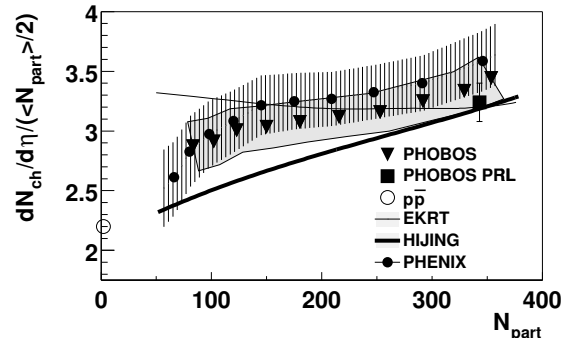


Figure 4. PHENIX and preliminary PHOBOS results for  $dN_{ch}/d\eta|_{\eta=0/1/2 N_{part}}$

energies. The new results show that 70% more particles are produced than at the SPS and 40% more than the extrapolation from  $\bar{p}p$  (also shown) would predict at  $\sqrt{s_{NN}} = 130$  GeV. This is strong evidence that particle production is not simply due to independent  $NN$  interactions. Instead, whatever process amplifies the production at SPS energies relative to  $pp$  collisions is even stronger at RHIC. At Quark Matter, the other three RHIC experiments presented new measurements [7,16,17] which are consistent with the original PHOBOS value within the stated systematic errors. We also show the predicted energy dependence from HIJING and an early EKRT calculation (both from [10]). Clearly, the increasing theoretical uncertainties emphasize the importance of varying the collision energy at RHIC.

At a fixed collision energy, one useful observable for understanding the relative role of hard processes is the variation of  $dN_{ch}/d\eta$  with  $N_{part}$ . The results of  $dN_{ch}/d\eta|_{\eta=0/1/2 N_{part}}$  vs.  $N_{part}$  is presented in Figure 4 which incorporates the results from PHENIX[18] and preliminary data from PHOBOS[6], which agree very well within systematic errors. These measurements cut off at  $N_{part} \sim 70$  since the systematic error on  $N_{part}$  grows rapidly below this (a situation which could be improved by colliding smaller nuclei, where even central events would have a smaller  $N_{part}$  than Au+Au). Interestingly, the data disfavors both of the leading predictions proposed before Quark Matter. Rather than being constant or rising linearly with  $N_{part}$ , as predicted by EKRT and HIJING respectively, the dependence on  $N_{part}$  looks most similar to that measured at the SPS and thus is in broad agreement with the Kharzeev-Nardi calculations[4].

One can also study the full distribution of  $dN_{ch}/d\eta$ , which is sensitive to all of the abovementioned physics effects but also gives insight into the role of longitudinal expansion and hadronic rescattering [19]. Preliminary PHOBOS data on  $dN_{ch}/d\eta|_{1/2 N_{part}}$  scaled by  $1/2 N_{part}$  is shown in Figure 5. As  $N_{part}$  increases, the distribution gets narrower. Indeed, forward particle production per participant actually *decreases*, suggesting that some fraction of particles are pulled back towards mid-rapidity via rescattering. Events generated with RQMD 2.4[20], which contains a substantial amount of such rescattering, qualitatively verifies this hypothesis. This seems to contradict models such as HIJING

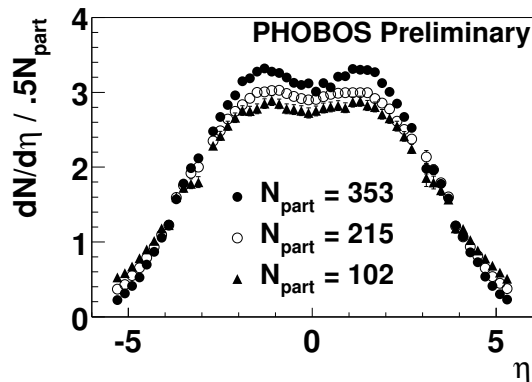


Figure 5. PHOBOS  $dN_{ch}/d\eta$  distributions scaled by the number of participants.

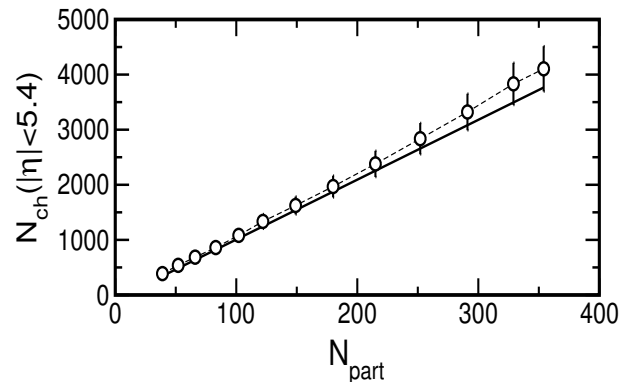


Figure 6. Preliminary PHOBOS data on total charged particle multiplicity vs.  $N_{part}$

which have no additional evolution of the system after the initial particles are produced, leading to no change in the particle production per participant outside of  $|\eta| > 3$ .

By integrating the  $dN_{ch}/d\eta$  distributions, PHOBOS also presented a measurement of the total number of charged particles as a function of  $N_{part}$ [19], shown in Figure 6. Results from a HIJING calculation are also presented and are consistent within the 10% systematic errors. This is remarkable considering the variety of possible physics effects that arise out of the collision dynamics.

#### 4. Transverse Energy

The measurement of transverse energy ( $E_T$ ) gives similar information as that of the charged multiplicity measurements, but  $E_T$  is also sensitive to the charged particle momentum spectrum. This gives us access to physics inaccessible to the previous measurements: the mean  $p_T$ , the initial energy density (through the Bjorken formula  $\epsilon = dE_T/d\eta/\pi R^2\tau$  [21]), and the effect of longitudinal flow ( $pdV$  work) on the evolving system.

At QM2001, PHENIX presented three results[16] pertaining to the produced transverse energy:  $dE_T/dN_{ch}$  vs.  $N_{part}$ ,  $dE_T/dN_{ch}$  vs.  $\sqrt{s_{NN}}$ , and  $dE_T/d\eta/\frac{1}{2}N_{part}$  vs.  $N_{part}$ . The transverse energy per charged particle is shown in Figure 7. It appears to be constant over the full range of centrality, which suggests that there is no dramatic modification of the particle spectra occurs when moving from peripheral to central collisions. It also suggests that the transverse energy at mid-rapidity should scale as the charged particle multiplicity. This is confirmed by the measurement of total transverse energy scaled by  $N_{part}$ [16]. However, while the transverse energy appears to scale simply with the number of particles, the transverse energy per charged particle as a function of  $\sqrt{s_{NN}}$ , shown in Figure 8, shows some surprising behavior. It appears that  $dE_T/dN_{ch}$  is the same at the AGS and at RHIC. However, the two experiments at the SPS (WA98 and NA49) suggest that this number might be the same, or perhaps larger, at SPS energies. This would seem to contradict the observations of the STAR experiment[22] at this conference that  $\langle p_T \rangle$  increases by 20% from SPS to RHIC energies. However, other results presented at the conference, e.g. jet-quenching, imply that particle production at RHIC shows new

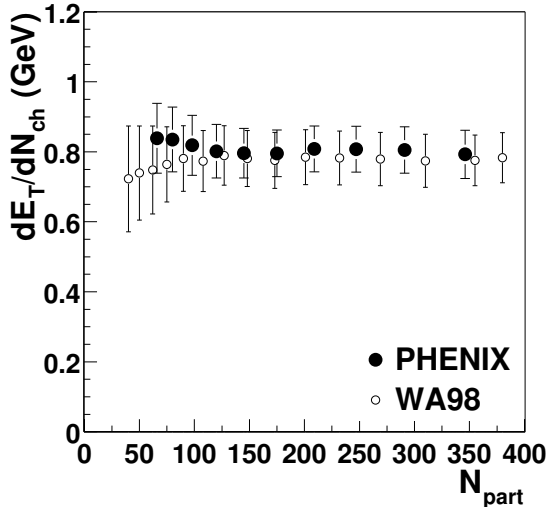


Figure 7. Preliminary PHENIX data and WA98 data on  $E_T/N_{ch}$  as a function of  $N_{part}$ .

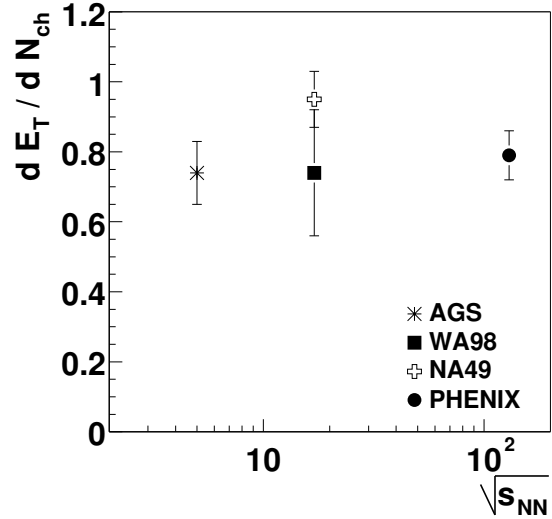


Figure 8.  $E_T/N_{ch}$  as a function of  $\sqrt{s_{NN}}$ . Along with AGS and SPS results, preliminary PHENIX data is shown.

features that might lead to deviations from expected behavior.

One of the most pressing questions at this conference concerns the energy density achieved in RHIC collisions. Using the Bjorken formula, NA49 extracted an initial energy density of  $\epsilon_{BJ} \approx 3.2 \text{ GeV}/\text{fm}^3$  [23]. Applying the same reasoning to the RHIC experiments would give a 70% increase. However, while the measurement of  $E_T$  seems straightforward, the Bjorken formula has theoretical uncertainties which do not decrease with beam energy. For example, the models of particle production based on parton saturation have formation times which vary as the inverse of the saturation scale  $\tau \sim \hbar/Q_s \sim .1 - .2 \text{ fm}$ . This would give an energy density of  $16 - 20 \text{ GeV}/\text{fm}^3$ , as shown in [4]. Clearly, further theoretical investigations are warranted in order to reduce the ambiguity in the concept of initial energy density.

## 5. Elliptical Flow

One of the most striking results from the initial round of RHIC results is the magnitude of the elliptical flow reported by the STAR experiment [24], which approaches the levels predicted by hydrodynamic calculations [25]. Since this initial result, the other experiments have confirmed this data and new information is now available about other aspects of this phenomenon [26–28].

As the two nuclei collide, the vector joining their centers defines the “reaction plane”. While one cannot directly measure the true reaction plane, subevent analysis is used to determine the experimental resolution obtained by using the measured particles themselves to estimate the collision angle  $\Psi$ ,  $n\Psi = \arctan(\sum_i \sin(n\phi_i) / \sum_i \cos(n\phi_i))$  [26]. Once  $\Psi$  is determined, one can extract the Fourier components  $v_1$  corresponding to directed flow, and  $v_2$  corresponding to the magnitude of elliptic particle flow. For a detector with limited acceptance, such as the PHENIX experiment with  $\Delta\phi = 180^\circ$ , one can use the

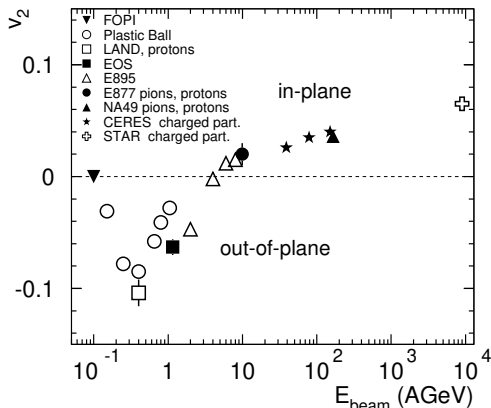


Figure 9. Energy dependence of  $v_2$ , showing data ranging from Bevalac to RHIC energies.

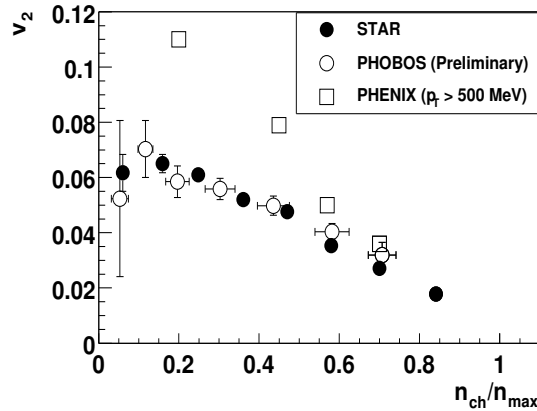


Figure 10. The STAR result compared with PHOBOS and PHENIX. PHENIX has a lower  $p_T$  cutoff of 500 MeV.

two-particle correlation function to extract  $v_2$ ,  $\frac{dN}{d\Delta\phi} \propto 1 + \sum_{n=1}^{\infty} 2v_n^2 \cos(n\Delta\phi)$  [28]. In principle, these two methods extract the same information. However, the correlation function method may be sensitive to other effects, e.g. jets or HBT, that would be missed by the other method.

The magnitude of  $v_2$  varies with the energy as well as the centrality of the collision. The centrality dependence is controlled by the eccentricity  $\epsilon$  of the nuclear overlap region. It has been shown [29,30] that when the system is dilute,  $v_2 \propto \epsilon \times dN/dy$ , where the rapidity density characterizes the probability of particles to rescatter. In the limit where the number of scatterings becomes large, only the initial geometry is important, so  $v_2 \propto \epsilon$ , and the proportionality constant can be predicted via hydrodynamic calculations[25]. The compiled data for the energy dependence of  $v_2$  is shown in Figure 9 (from [31]). The large anti-flow (squeeze-out) observed in low-energy nuclear collisions is seen to change sign at  $\sqrt{s_{NN}} = 4\text{GeV}$ , turning into a continuous logarithmic rise of  $v_2$  all the way to RHIC energies. It is interesting to note that  $v_2$  at RHIC is approximately 60% higher than at the SPS, similar to the 70% increase in  $dN_{ch}/d\eta$  already mentioned.

Since STAR's original result [24], three of the four RHIC experiments have measured the dependence of  $v_2$  with centrality, as shown in Figure 10. Both STAR and PHOBOS measure the event with full azimuthal acceptance and comparable event plane resolution. PHENIX uses the correlation function method and has a lower  $p_T$  cutoff of 500 MeV, both of which may explain why the PHENIX  $v_2$  result is somewhat higher than the other two.

The  $p_T$  dependence of  $v_2$  appears to both support the hypothesis that the central region of RHIC collisions shows hydrodynamic behavior, as well as suggest the appearance of jet quenching. STAR and preliminary PHENIX data[28] on  $v_2(p_T)$  are shown in Figure 11 and are in broad agreement, at least for the basic trend. Calculations given in [32] have reproduced the STAR data up to  $p_T = 2\text{ GeV}$ . The same calculations also predict  $v_2$  for identified pions and protons and finds that protons only have non-zero flow above  $p_T \sim 400\text{ MeV}$ . Also shown in Figure 11 are calculations of jet quenching which incorporate the

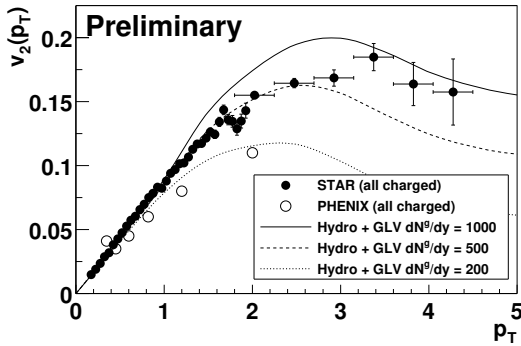


Figure 11. Comparison of charged particle  $v_2(p_T)$  with GLV calculations including hydro and jet-quenching. Preliminary data from PHENIX and STAR are shown.

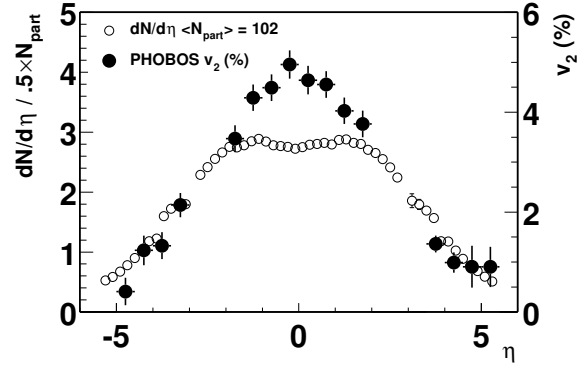


Figure 12.  $v_2$  (from PHOBOS) as a function of  $\eta$  overlaid on top of  $dN_{ch}/d\eta$  for  $N_{part} = 102$  (see Figure 5).

geometry of the collision zone[33]. They find that quenching has a dramatic effect on  $v_2$  at very high- $p_T$ . Both of these are consistent with the preliminary STAR data[26].

PHOBOS presented data for  $v_2$  vs.  $\eta$  all the way to  $\eta = 5.4$ [27], shown in Figure 12. Although results from three-dimensional hydrodynamic calculations are not available, one can still ask if  $v_2$  away from mid-rapidity scales with  $dN_{ch}/dy$ , which is similar to  $dN_{ch}/d\eta$  in this region. Figure 12 shows the PHOBOS data overlaid with the most peripheral distribution from Figure 5. Following a suggestion by Manly[34], one can scale the multiplicity distribution to roughly match  $v_2$  for  $|\eta| > 2$ , to find remarkable agreement in the shape. The sharper peak in the flow distribution might simply be due to the flattening of the multiplicity distribution near  $\eta = 0$  suggested by the Jacobian shown in equation 1.

## 6. Conclusions

We have seen that the global and flow observables measured at RHIC all show non-trivial collective behavior which was not predicted by any model. Indeed, the presence of the strong elliptic flow and the evolution of  $dN_{ch}/d\eta$  at the forward and backward rapidities show the effect of rescattering processes that models such as HIJING do not incorporate. With the upcoming 200 GeV run at RHIC, there are great opportunities to push our understanding even further. However, it should not be forgotten that extensive species and energy scans will be needed to make sure that we have an appropriate understanding of the basic features of particle production before we make detailed interpretations of the high statistics RHIC data.

## 7. Acknowledgements

The author would like to thank the organizers of Quark Matter 2001 for a stimulating experience on all fronts. Thanks to the RHIC collaborations and especially H. Appelshauser, M. Chiu, R. Lacey, A. Milov, I. Park, R. Snellings, X.-N. Wang, and S.



White for providing results for this article.

## REFERENCES

1. Proceedings of “Quark Matter 2001”, to appear in Nucl. Phys. A (referred to here as “these proceedings”).
2. C. Adler, A. Denisov, E. Garcia, M. Murray, H. Strobele and S. White, nucl-ex/0008005.
3. R.J. Glauber, in Lectures in Theoretical Physics, edited by W.E. Brittin and L.G. Dunham (Interscience, N.Y., 1959), Vol. 1, 315.
4. D. Kharzeev and M. Nardi, nucl-th/0012025.
5. A. Denisov, these proceedings.
6. J. Katzy, these proceedings.
7. F. Videbeck, these proceedings.
8. K. Eskola, these proceedings.
9. M. Gyulassy and X.N. Wang, Phys. Rev. **D44** 3501 (1991).
10. X. Wang and M. Gyulassy, nucl-th/0008014.
11. F. Abe et al., Phys. Rev. **D41**, 2330 (1990).
12. B. B. Back *et al.*, Phys. Rev. Lett. **85**, 3100 (2000).
13. M. M. Aggarwal *et al.*, Eur. Phys. J. C **18**, 651 (2001).
14. WA97 and NA57 Collaborations, F. Antinori et al., Preprint CERN-EP-2000-002.
15. K. J. Eskola, K. Kajantie, P. V. Ruuskanen and K. Tuominen, Nucl. Phys. **B570**, 379 (2000).
16. A. Milov, these proceedings.
17. T. Ullrich, private communication.
18. K. Adcox *et al.*, nucl-ex/0012008.
19. A. Wuosmaa, these proceedings.
20. H. Sorge, nucl-th/9905008.
21. J. D. Bjorken, Phys. Rev. D **27**, 140 (1983).
22. M. Calderón, these proceedings.
23. S. Margetis *et al.* Phys. Rev. Lett. **75**, 3814 (1995).
24. K. H. Ackermann *et al.*, Phys. Rev. Lett. **86**, 402 (2001).
25. J.-Y. Ollitrault, Phys. Rev. D **46**, 229 (1992).
26. R.J. Snellings, these proceedings.
27. I.C. Park, these proceedings.
28. R. Lacey, these proceedings.
29. S. A. Voloshin and A. M. Poskanzer, Phys. Lett. B **474**, 27 (2000).
30. H. Heiselberg and A. Levy, Phys. Rev. **C59**, 2716 (1999).
31. H. Appelshauser, these proceedings.
32. P. F. Kolb, P. Huovinen, U. Heinz and H. Heiselberg, Phys. Lett. B **500**, 232 (2001).
33. M. Gyulassy, P. Levai and I. Vitev, Nucl. Phys. B **571**, 197 (2000).
34. S. Manly, private communication.